minerals

MDPI

Article

Quantitative Evaluation of Crystalline and Amorphous Phases in Clay-Based Cordierite Ceramic

Zdeněk Klika [1,*], Marta Valášková [2], Lucie Bartoňová [1] and Petra Maierová [3]

[1] Department of Chemistry, VŠB-Technical University of Ostrava, 17. listopadu 15, 708 00 Ostrava-Poruba, Czech Republic; lucie.bartonova@vsb.cz
[2] Institute of Environmental Technology, VŠB-Technical University of Ostrava, 17. listopadu 15, 708 00 Ostrava-Poruba, Czech Republic; marta.valaskova@vsb.cz
[3] Department of Thermal Engineering, VŠB-Technical University of Ostrava, 17. listopadu 15, 708 00 Ostrava-Poruba, Czech Republic; petra.maierova@vsb.cz
* Correspondence: zdenek.klika@vsb.cz; Tel.: +420-723-589-655

Received: 20 November 2020; Accepted: 13 December 2020; Published: 14 December 2020

Abstract: An innovative chemical quantitative mineral analysis (CQMA) was successfully tested on a cordierite-based clay ceramic sample to quantify crystalline and amorphous components. The accuracy of this method was demonstrated on an added module to the CQMA program that used oxide formulas of amorphous phases obtained by energy dispersive X-ray spectroscopy (EDS) microprobe chemical analysis. This CQMA method was tested for three variants calculated using chemical analysis, i.e., X-ray diffraction (XRD) identification of crystalline (cordierite and enstatite) and amorphous phases by scanning electron microscopy (SEM)/EDS texture and microanalyses. The test results from CQMA suggest their application possibilities as well as the limits of their utilization.

Keywords: cordierite ceramics; crystalline and amorphous phases; CQMA; XRD; XRF; SEM/EDS; critical evaluation

1. Introduction

Clays and clay minerals are used in ceramic industries largely because of their contribution to the plasticity in ceramic mixtures and the density of the body at firing temperatures. Conventional methods for the synthesis of cordierite ceramics include solid-state sintering of individual oxides of the chemical composition of cordierite $2MgO\text{-}2Al_2O_3\text{-}5SiO_2$. The natural raw materials, kaolinite and talc, containing oxides MgO, Al_2O_3, and SiO_2, are often used to fabricate cordierite ceramics [1]. Cordierites have also been sintered from clay mineral mixtures containing vermiculite [2,3]. Cordierite $Mg_2Al_4Si_5O_{18}$ rapidly crystallizes from a glass of stoichiometric oxide composition to a well-defined hexagonal crystalline structure [4]. Cordierite ceramics prepared in the laboratories and industry have been found to be strongly dependent on the composition of raw materials and the presence of impurities. Therefore, mullite, corundum, spinel, forsterite, clinoenstatite, and cristobalite secondary crystalline phases are often present together with a glassy phase [5]. The glasses that have been investigated contained substantial amounts of TiO_2 as the nucleating agent [6]. Amorphous phases are commonly found in ceramics [1,3], slags [7,8], fly ash [9,10], cements and concretes [11,12], and their evaluation is performed by various methods. The group of analytical methods that provide very important information about mineral phases includes microscopic methods, the most common of which is electron microscopy [13,14].

Scanning electron microscopy (SEM) enables the characterization of the morphology, shape, size, and particle distribution in materials and moreover the possibility of studying the amorphous phase, cross-section pores, and the computer image analysis [15,16]. For analyses of elemental composition,

SEM is supplemented using the energy dispersive X-ray spectroscopy (EDS) technique that enables identification of phases that occur with very small diameter (μm) [17,18].

Generally, qualitative and quantitative determination of mineral phases is performed by using X-ray diffraction (XRD) methods [19]. Currently, XRD supplemented by Rietveld's techniques [20–22] to evaluate full profiles of all diffraction patterns is the most accurate procedure for the quantification of crystalline mineral phase by using the QXRD-Rietveld method. For the materials containing an amorphous phase not exhibiting defined Bragg reflection, the QXRD-Rietveld method should be supplemented by using internal or external standards [23]. Currently, added spikes of ZnO, Al_2O_3, or, for example, Si, etc. as the internal standards [24], provide good results using the QXRD-Rietveld method [22]. Recently, the identification and quantitative determination of amorphous and crystalline phases has been performed by the QXRD-Rietveld method and synergic SEM, EDS, and multispectral image analysis [25]. However, the accuracy of the QXRD-Rietveld method depends on the crystallinity of the present phases, because "X-ray amorphous" phases cannot be directly measured. The accuracy of the methods was tested by the external standard method with known amounts of glass [26]. The quantitative amount of amorphous phase was compared with the results obtained using the QXRD-Rietveld method with internal and external standards, method of linear calibration model (LCM), Partial Or No Known Crystal Structure (PONKCS) method, and degree of crystallinity (DOC). The results highlighted the following significant conclusions: (a) if the intensity ratio of the amorphous content in the diffraction pattern is not obvious, some indirect method should be used (e.g., internal or external standard); (b) all methods described in this study can practically be used for the determination of the concentration of the amorphous component with similar accuracy as in the case of crystalline phases [27].

A different approach to quantitative analysis for calculating mineral percentages in various materials is also based on the recalculation of bulk chemical analysis or other parameters of the analyzed sample. In principle, all these methods integrate the XRD data of identified minerals with relevant chemical analysis and refinement of the mineral composition calculated using the mathematical approach [28–30]. The recalculation procedure of the chemical analysis results to mineral composition using the method of singular value decomposition (SVD) has been proposed, however, it was found not always feasible due to the variability of mineral composition [31]. Similarly, an alternative rational mineralogical analysis has been used to recalculation chemical analysis to quantitative analysis of minerals in ceramics [32] and chemical quantitative mineral analysis (CQMA) method for materials containing crystalline phases [33].

This study presents the newly modified CQMA method in combination with XRF, XRD, and EDS methods to obtain the quantitative analysis of crystalline and non-crystalline components in a cordierite ceramic sample (CCS) obtained from a larger set of cordierite ceramic [3].

2. Materials and Methods

The cordierite ceramic sample (CCS) was obtained from kaolinite (K) and vermiculite (Ver) with the K/Ver mass ratio of 1:1 in a mixture sintered for 1 h at 1300 °C (more details are in our previous paper [3]). The Ver sample was milled in a cylindrical agate container for 15 min at 550 rpm using an agate planetary mill Fritsch Pulverisette 5, and then was prepared to the fraction <40 μm from sieve. The ceramic K/Ver mixture was homogenously mixed in a bottle at 40 rpm for 1 h (Heidolph Reax overhead shaker, REAX 20/4, Merck Company, Kenilworth, NJ, USA), and then milled for 15 min at 550 rpm in an agate planetary mill Fritsch Pulverisette 5. The mixture sample (3 g) was gently pressed by hand in a porcelain combustion boat, and then sintered in an electrical laboratory furnace LH15/13 for 1 h at 1300 °C. The heating rates were 10 °C/min up to 1000 °C and 2 °C/min until the sintering temperature of 1300 °C was achieved. The sample were left at this temperature for 1 h, and after that it was slowly cooled to room temperature. The ceramic sample for ED-XRF and XRD analysis was ground in a planetary ball mill under the same conditions as the mixture, and then manually pulverized with an agate mortar and pestle.

Kaolinite originates from the kaolin in the Pilsen Basin from locality Chlumčany (supplied by LB Minerals, Ltd., Horní Bříza, Czech Republic) and vermiculite originates from the Paraíba state, northeast region of Brazil (supplied by Grena, a.s., Veselí nad Lužnicí, Czech Republic).

For the SEM and EDS microanalysis study, the cordierite samples with grain size of about 2–5 mm were embedded in epoxy, dry polished, and then were plated with a 35 nm Cr layer by plasma sputtering.

The chemical elemental analysis was performed using the energy dispersive X-ray fluorescence (ED-XRF) spectrometer SPECTRO XEPOS (Spectro Analytical Instruments, Kleve, Germany). Prior to analysis, the measured CCS was finely ground to a particle size below 40 μm. For the XRF analysis, reference samples of metamorphic rocks based on clay minerals were used.

The XRD analyses were carried out on a Rigaku SmartLab diffractometer (RIGAKU, Tokyo, Japan) working in the symmetrical Bragg–Brentano geometry and with the CoKα radiation (λ_1 = 0.178892 nm and λ_2 = 0.179278 nm). The acceleration voltage on the sealed tube was 40 kV, the current was 40 mA. The diffracted intensities were recorded using a one-dimensional (1D) silicon strip detector D/teX Ultra 250 in the 5–80° 2θ range with a speed of 0.5°/min and a step size of 0.01°.

The CQMA method recalculates the percentages of minerals to the percentages of elemental oxides (e.g., SiO_2, Al_2O_3, Fe_2O_3, FeO, etc.) and vice versa, i.e., recalculation the percentages of element oxides to percentages of selected minerals (Figure 1). Selected minerals identified, for example, by XRD or optical methods have to also be characterized by their crystallochemical/oxide formulas [33]. The CQMA program is equipped with a wide database of fixed crystallochemical/oxide formulas (e.g., $MgSiO_3$/MgO SiO_2) and also formulas that can be modulated via their isomorphic substitution (e.g., micas, montmorillonites, vermiculites, etc.).

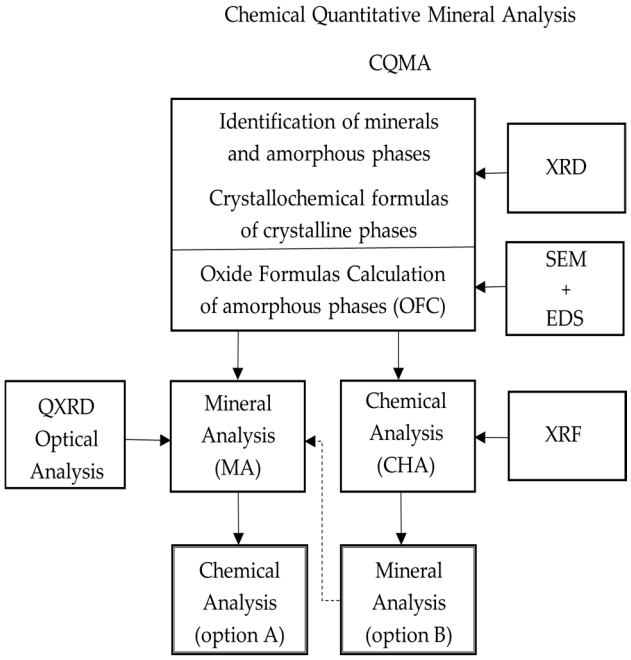

Figure 1. Simplified scheme of the chemical quantitative mineral analysis (CQMA) method for the calculation of bulk chemical composition from mineral analyses (option A) and for the calculation of minerals from bulk chemical analyses (option B). (Scheme is adopted from Klika et al. [33]).

The oxides of elements were calculated from minerals (i.e., analytes $c_{i,calc}$) according to Equation (1) using the CQMA (option A) as:

$$c_{i,calc} = \sum_{j=1}^{m} c_{i,j} \times w_j \quad (1)$$

where $c_{i,calc}$ is the calculated i-th element oxide (wt%) of the sample, $c_{i,j}$ is the percentage (wt%) of the i-th element oxide in the j-th mineral phase, w_j is the weight fraction of the j-th mineral in the sample, and m is the number of calculated minerals.

The weight fraction of the i-th element oxide in the j-th mineral $c_{i,j}$ is calculated from the crystallochemical formula of the j-th mineral.

The calculation of the weight fractions of the j-th mineral (w_j) was calculated by Equation (2) using the CQMA (option B) as:

$$\sum_{i=1}^{n}\left(c_{i,exp} - \sum_{j=1}^{m} c_{i,j} \times w_j\right)^2 = min \quad (2)$$

where $c_{i,exp}$ is the i-th element oxide in the sample (wt%) determined by bulk chemical analysis, min is the minimum calculated value of the sum of squares, and n is the number of element oxides in the bulk chemical analysis used for the calculation; condition necessary for the CQMA calculation, $n \geq m$.

The calculation of the weight fraction (w_j) of the j-th mineral in the sample from Equation (2) is performed using the least squares CQMA method. The feedback calculation of the chemical analysis $c_{i,calc}$ from the calculated minerals w_j is then performed from Equation (1). Subsequently, the $c_{i,exp}$ and $c_{i,calc}$ are critically compared using their differences $DIFF_i = c_{i,exp} - c_{i,calc}$. If $DIFF_i$ for some i-th element oxides are too high (positive or negative), they can be attributed to some incorrect input data, for example, to the bulk chemical analysis, crystallochemical formula, or identified minerals. After critical evaluation, these data can be reanalyzed or additional data can be added, and then the calculation is repeated. More details about this method and also verification of CQMA calculated data on the data of 6 international standards has already been published and critically evaluated elsewhere [33].

Scanning electron microscopy (SEM) of the samples, monitoring morphology, and rough composition of the determined phases were performed on polished sections using an FEI Quanta-650 FEG autoemission electron microscope (Waltham, MA, USA) from Thermo Fischer Scientific. Photomicrographs were taken using a backscattered electron (BSE) detector (Termo Fischer Scientific, Brno, Czech Republic) in chemical gradient mode.

The chemical composition of the minerals was verified using an EDAX Galaxy energy dispersive spectrometer (Edax Amentek, USA). EDS microanalyses were performed with the correction by external polished microanalysis standards of aluminosilicate minerals by SPI Supplies (USA). Identification of spectral lines was performed by spectral deconvolution using the holographic peak deconvolution function.

3. Results

3.1. Chemical and X-ray Diffraction (XRD) Phase Analyses

The chemical composition of CCS was obtained using the bulk chemical analysis (ED-XRF) (Table 1). The concentrations of elements were converted to the concentrations of stoichiometric oxides (wt%); Fe was recalculated to FeIII as Fe_2O_3.

Table 1. Bulk chemical analysis of cordierite ceramic sample (CCS) (wt%).

SiO_2	TiO_2	Al_2O_3	Fe_2O_3	MnO	MgO	CaO	Na_2O	K_2O	Total
52.95	0.81	25.27	4.44	0.05	13.26	0.70	0.21	2.09	99.78

The chemical analysis (CHA) was completed by XRD identification and quantitative analyses of mineral phases. The XRD pattern of ceramic CCS shows cordierite (PDF card no. 01-082-1884) and enstatite (PDF card no. 00-019-0768) (Figure 2).

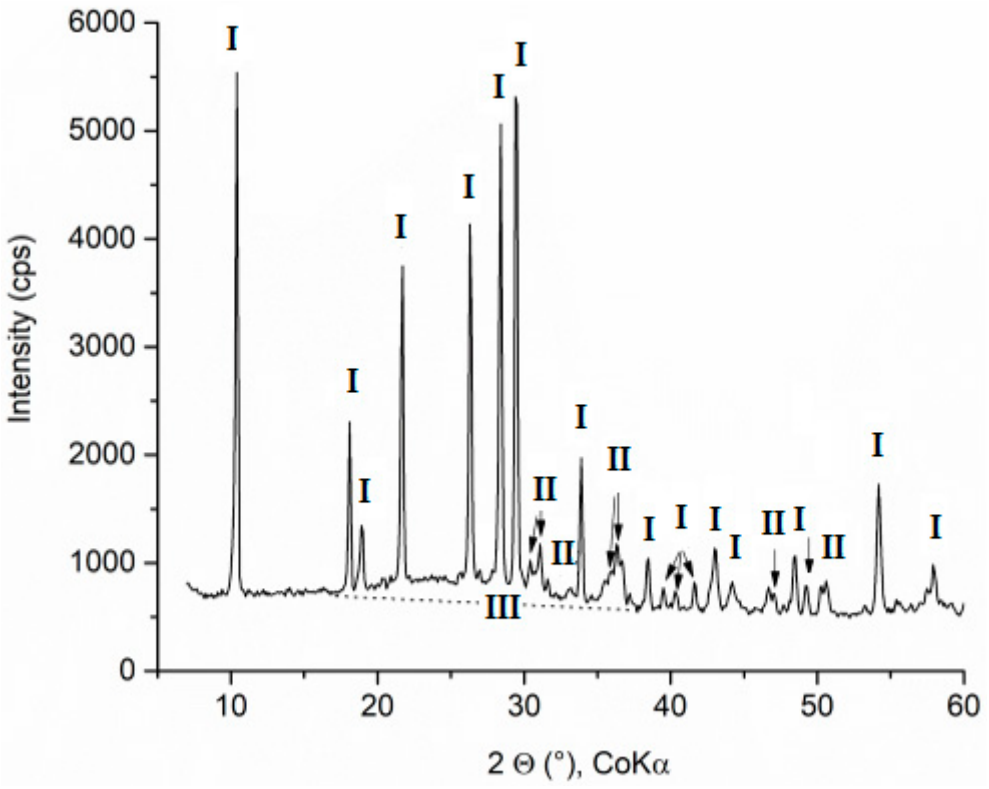

Figure 2. X-ray diffraction (XRD) pattern of the ceramic CCS. I, cordierite I; II, enstatite; dotted line separates a non-crystalline phases III area from the background.

An "amorphous" halo from about 20° to 35° (2 θ) of the amorphous phases is marked from the background by the dotted line. The quantitative percentages of cordierite (95 ± 2.5 wt%) and enstatite (5 ± 2.5 wt%) were calculated by using the reference intensity ratio (RIR) method from the not overlapping diffractions [34]. The crystallochemical formulas of cordierite $Ca_{0.10}Mg_{1.90}Fe(III)_{0.40}Al_{3.60}Si_{5.00}O_{18.00}$ and enstatite $MgSiO_3$ were selected from our previous work [3] and are similar to those reported by Balassone et al. [35].

3.2. Scanning Electron Microscopy (SEM)

The CCS morphology was studied by scanning electron microscopy (SEM), as shown in Figure 3. At this lower magnification (1600×) pseudohexagonal crystals of cordierite (phase I) can be well differentiated from an amorphous matter (III) that consists of two different phases, III/1 and III/2 (Figure 3a). Enstatite identified using XRD pattern may correspond to the phase II with needle habitus (*ei*, enstatite inclusion) in Figure 3b.

The crystalline enstatites occur in pseudohexagonal crystals of cordierite I and in amorphous phase III/1 but are not observed in phase III/2 (Figure 3b). Phases I and III/2 are encapsulated in the phase III/1 around them. Except for enstatite inclusions (*ei*), other small glassy inclusions (*oi*) occur, namely, in amorphous phase III/1 but not observed in phase III/2. The chemical composition of both types of these inclusions and their identification by EDS is rather complicated (Figure 3b). This is because at least one of the dimensions of these inclusions is smaller than 1–2 μm, while the emitted ray of EDS is simultaneously analyzing the surrounding area of the observed objects with diameter of about 5 μm (Figure 3b).

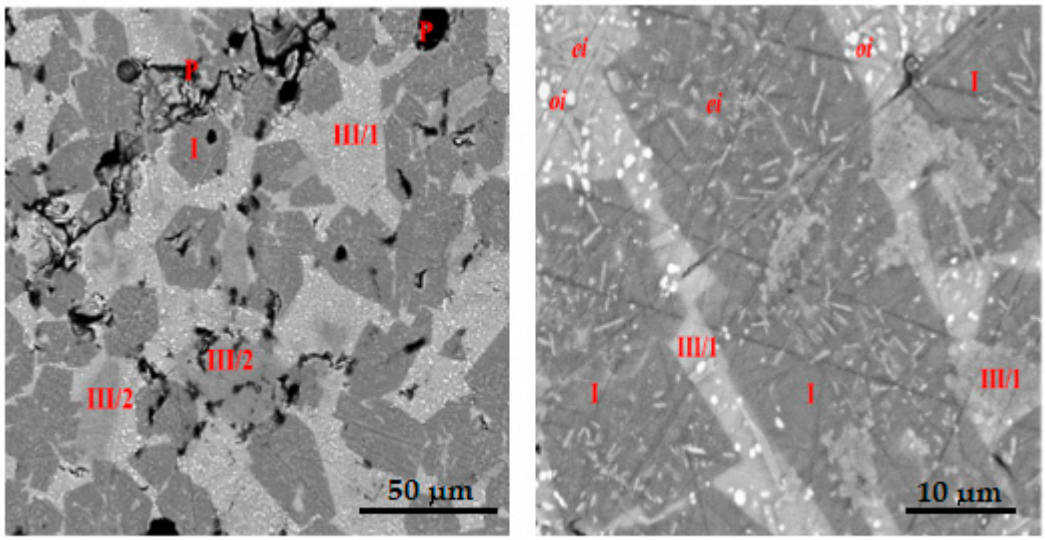

Figure 3. Texture of CCS. (**a**) I, cordierite; III/1, amorphous phase; III/2, amorphous phase; P, pores; (**b**) Inclusions in texture of CCS. I, cordierite with II, enstatite inclusion (*ei*) and III/1, amorphous phase (*oi,* other not identified inclusion and *ei*).

3.3. X-ray Energy Dispersive Spectroscopy (EDS) and Calculated Oxide Formula Coefficients

The SEM observations confirmed that the highest percentage relates to cordierite (Phase I), followed by the amorphous phases III/1 and III/2 (Figure 3a). The microanalysis of these phases was obtained by energy dispersive X-ray apectroscopy (EDS) on 10 samples of cordierite (phase I) and 10 samples of amorphous phase III/1. From amorphous phase III/2, only seven analyses were performed with the view of lower % representation. Positions/locations of these microanalyses conducted are depicted in Figure 3a and their calculated average values of $\overline{c_i}$ and standard deviations s_i are listed (Table 2).

Table 2. Microprobe analyses of elemental oxides determined by energy dispersive X-ray spectroscopy (EDS) and calculated oxide formula coefficient (OFC_i).

Oxides	Molecular Weight (g/mol)	Cordierite I				Amorphous Phase III/2				Amorphous Phase III/1		
		$\overline{c_i}$	s_i	OFC_i	$c_{i,cord}$	$\overline{c_i}$	s_i	OFC_i	$c_{i,enst}$	$\overline{c_i}$	s_i	OFC_i
		(mol%)				(mol%)				(mol%)		
SiO_2	60.1	57.7	1.1	10.0	55.55	46.0	3.7	10.0	50.00	68.39	1.83	10.0
TiO_2	79.9					2.57	0.3	0.56		1.71	0.24	0.25
Al_2O_3	101.9	17.7	0.82	3.10	20.00	12.1	3.2	2.66		11.90	0.98	1.74
Fe_2O_3	159.7	1.73	0.30	0.30	2.22		0.2	0.21		3.14	0.37	0.46
MgO	40.31	20.8	0.41	3.60	21.1	36.4	7.7	7.92	50.00	7.38	0.92	1.08
CaO	56.08	0.87	0.90	0.15	1.11		0.6	0.10		3.20	0.27	0.47
Na_2O	61.98									1.02	0.10	0.15
K_2O	94.02	1.09	0.19	0.19		1.33	0.3	0.29		3.24	0.33	0.48
Total		100.0			99.98	99.9				100.0		

Note: $\overline{c_i}$, average percentage of elemental oxides calculated from n samples determined by EDS microanalyses and calculated for I, III/1 and III/2 phases (Figure 3a); $c_{i,cord}$ and $c_{i,enst}$, oxide percentage of oxide elements calculated from crystallochemical formulas of cordierite ($Ca_{0.1}Mg_{1.90}Fe(III)_{0.40}Al_{3.60}Si_{5.00}O_{18}$) and enstatite ($MgSiO_3$), respectively. Standard deviation $s_i = \sqrt{\frac{1}{n-1}\sum_1^n (x_i - \overline{x})^2}$, where n is the number of determined samples.

While amorphous phase III/1 is nearly homogeneous in terms of bulk chemical composition, amorphous phase (III/2) is heterogeneous corresponding higher standard deviations s_i. The chemical microanalyses of phases I, III/1, and III/2 are contaminated by inclusions of other phases marked as *ei* in phase I, *ei* and *oi* in phase III/1, and *ei* inclusion in phase III/2 (Figure 3a,b). The proportion of

these other phases can hardly be estimated; nevertheless, it can be deduced that the chemical analyses do not correspond with the pure phases of cordierite and amorphous phases III/1 and III/2 without inclusions (Table 2).

For the relevant *i*-th oxides of phases I, III/1, and III/2, $\overline{c_i}$ values were used for the calculation of their oxide formula coefficient (OFC_i) using Equations (3) and (4) as follows:

$$OFC_i = \overline{c_i} \times f_{SiO2} \quad (3)$$

$$f_{SiO2} = \frac{10.00}{\overline{c_{SiO2}}} \quad (4)$$

where f_{SiO2} is correction factor used for the recalculation of all *i*-th OFC_i values to the relation to value OFC_{SiO2} = 10.00 for each phase (If any number instead of constant 10.00 is used, then the *i*-th oxides of the elements will preserve the same ratio with each other and the final calculation of the crystalline or amorphous percentages calculated by CQMA will not be affected); $\overline{c_{SiO2}}$ is average concentration of SiO_2. f_{SiO2} = 0.1734 for phase I; f_{SiO2} = 0.2174 for phase III/2; f_{SiO2} = 0.1462 for phase III/1.

Average *EDS* elemental microanalyses $\overline{c_i}$ of cordierite I, amorphous phases III/1 and III/2 are recalculated on OFC_i (Table 2). The $\overline{c_i}$ values of cordierite I are compared with $c_{\mathrm{i,cord}}$ of cordierite ($Ca_{0.1}Mg_{1.90}Fe^{3+}{}_{0.40}Al_{3.60}Si_{5.00}O_{18}$) and $\overline{c_i}$ of amorphous phases III/1 and III/2 with $c_{\mathrm{i,enst}}$ of enstatite $MgSiO_3$ (Table 2).

The comparison of cordierite oxides ($\overline{c_i}$ and $c_{i,cord}$) indicates a very good agreement. Microanalyses ($\overline{c_i}$) of amorphous phases III/1 and III/2 as compared with the $c_{i,enst}$ of enstatite are different. Nevertheless, the chemical composition of III/2 phase is closer to enstatite due to their high % of MgO. However, high standard deviations, s_i, signalize high heterogeneity and enstatite cannot be assumed. Therefore, for III/1 amorphous phase the calculation of $c_{i,enst}$ was not necessary.

The concentrations of elemental oxide maps are collected by SEM/EDS system (Figure 4). The distributions of cordierite I, as well as amorphous phases III/1 and III/2 are shown on the photo (see left side of this figure). The resolution of element oxide concentrations in the phases can be found according to the intensity of their coloration. A higher intensity (lighter color) corresponds to higher contents of the element. The results are summarized in the following points:

- The cordierite phase I contains the highest % Al_2O_3 and the lowest % CaO, and Fe_2O_3;
- Amorphous phase III/1 contains the highest % CaO, Na_2O, K_2O, SiO_2, TiO_2, and Fe_2O_3;
- Amorphous phase III/2 contains the highest % MgO and the lowest % Al_2O_3.

OFC for individual phases I, III/2, and III/1 were compiled from their OFC_i data (Table 3).

Table 3. Compiled oxide formula coefficients (*OFC*) for calculated phases.

Phases	Oxide Formula Coefficient (*OFC*)
Cordierite I	$10SiO_2$ $3.10Al_2O_3$ $0.30Fe_2O_3$ 3.60MgO 0.15CaO $0.19K_2O$
Amorphous phase III/1	$10.0SiO_2$ $0.25TiO_2$ $1.74Al_2O_3$ $0.46Fe_2O_3$ 1.08MgO 0.47CaO $0.15Na_2O$ $0.48K_2O$
Amorphous phase III/2	$10SiO_2$ $0.56TiO_2$ $2.66Al_2O_3$ $0.21Fe_2O_3$ 7.92MgO 0.10CaO $0.29K_2O$

The results in Figure 4 agree well with the determined % contents of individual oxides of elements ($\overline{c_i}$) in Table 2.

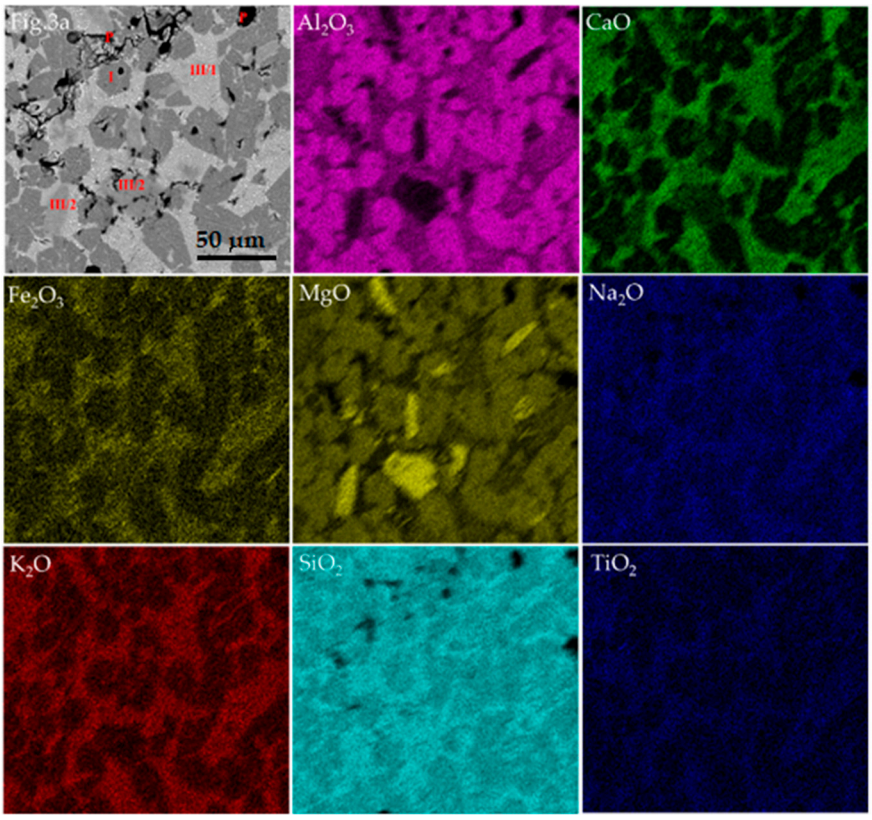

Figure 4. Maps of the elemental oxides' concentration (%) in various phases.

3.4. Calculation of Minerals Percentages Using CQMA (Option B)

The CQMA program (option B) for the calculation of mineral percentages of analyzed sample used the following input data: (a) bulk chemical analysis (Table 1), (b) identified crystalline minerals by XRD, and (c) their crystallochemical formula obtained from XRD database or from compiled oxide element formula obtained using the microanalysis of analyzed sample (Table 3). The CQMA calculations were performed for the following different Variants 1–3:

Variant 1

Crystallochemical/oxide formulas were the following:

- Cordierite, $Ca_{0.1}Mg_{1.90}Fe^{3+}{}_{0.40}Al_{3.60}Si_{5.00}O_{18}$/5.00$SiO_2$ 1.80Al_2O_3 0.20Fe_2O_3 1.90MgO 0.10CaO;
- Enstatite, $MgSiO_3$/MgO SiO_2.

For variant 1 and the following variant 2 the crystallochemical formulas for cordierite and enstatite have already been given and discussed in Section 3.1. From bulk chemical analysis (Table 1) all percentages of Al_2O_3, Fe_2O_3, CaO, MgO, and part of SiO_2 were included in identified crystalline phases (cordierite and enstatite), while the surplus of SiO_2 (7.56%) and all percentages of TiO_2 (0.81%), Na_2O (0.21%), and K_2O (2.09%) were included in non-crystalline phase. For this purpose, the calculation by CQMA (option B) was used and maximal possible percentages of crystalline minerals (89.0%) and minimal percentages of amorphous phase (10.7%) were obtained. Then, the percentages of element oxides obtained from non-crystalline phase were recalculated to the oxide formula 10.0SiO_2 0.81TiO_2 0.27Na_2O 1.72 K_2O.

Variant 2

Crystallochemical/oxide formulas were the following:

- Cordierite, $Ca_{0.1}Mg_{1.90}Fe^{3+}{}_{0.40}Al_{3.60}Si_{5.00}O_{18}$/5.00$SiO_2$ 1.80Al_2O_3 0.20Fe_2O_3 1.90MgO 0.10CaO;
- Enstatite, $MgSiO_3$/MgO SiO_2;

- Amorphous phase III/1, $10SiO_2$ $0.25TiO_2$ $1.74Al_2O_3$ $0.46Fe_2O_3$ $1.08MgO$ $0.47CaO$ $0.15Na_2O$ $0.48K_2O$;
- Amorphous phase III/2, $10SiO_2$ $0.56TiO_2$ $2.66Al_2O_3$ $0.21Fe_2O_3$ $7.92MgO$ $0.10CaO$ $0.29K_2O$.

For the variant 2, the crystallochemical formulas of cordierite and enstatite from variant 1 were used. In addition to this, for the calculation of amorphous phase III/1 and the other amorphous phase III/2, the compiled *OFC* were used (Table 3).

Variant 3

OFC of cordierite I, amorphous phase III/1 and amorphous phase III/2 (Table 3) were used for calculation (Table 3).

Calculated results from XRD analysis and variants 1–3 of CQMA (option B) are given in Table 4 and graphically shown in Figure 5.

Table 4. Percentages of determined phases (wt%) using the CQMA method for variants 1–3 and the XRD (RIR) method.

Phases	XRD	CQMA (Option B)		
		Variant 1	Variant 2	Variant 3
Cordierite I	95.0	82.3	64.43	70.4
Enstatite II/or *ei*	5.0	6.7	6.02	n.d.
Amorphous phase III/1	n.d	10.7	22.70	14.7
Amorphous phase III/2	n.d.	n.d.	7.35	14.9
Total	100.0	99.7	100.5	100.0
P1	19.0	12.3	10.6	-
P2	n.d	8.3	3.1	-

Note: P1 = % cordierite/% enstatite; P2 = (% cordierite + % enstatite)/(% total amorphous phases); n.d., not determined.

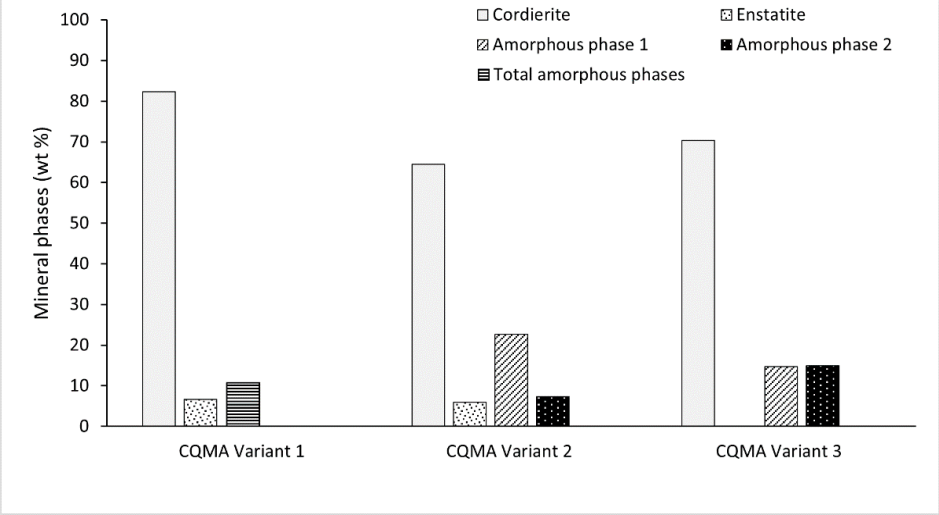

Figure 5. Comparison of calculated percentages for variants 1–3 determined by CQMA (option B).

4. Discussion

Results of variant 1 can be considered to be indicative, showing a relation with the total maximal content of both crystalline phases (cordierite and enstatite) and minimum content of total amorphous phase, which is afterwards documented by percentages of phase contents calculated from variant 2 and variant 3.

Unlike variants 1 and 3, variant 2 enables use of two *OFC* phase formulas III/1 and III/2 calculated from averages of microanalyses (Table 2). The *OFC* formulas used for the calculation of both amorphous phases III/1 and III/2 are given in Table 3. The added amorphous phase III/2 shows that this phase

(unlike amorphous phase III/1) is very heterogeneous and is characterized for some elemental oxides (e.g., Al_2O_3 and MgO) by high standard deviations (Table 2). Calculated percentages of phases I, II, III/1, and III/2 (Table 4) are in a good agreement with compared phases in Figure 3a,b. Phase II (enstatite) was identified only by XRD and in Figure 3b was denoted as inclusion (*ei*) in all phases of the analyzed sample.

In variant 3, the same *OFC* phase formula of amorphous phases III/1 was used for the calculation of phases, similar to the case of the previous variant 2. For cordierite (I), the *OFC* formula (Table 3) partially includes the inclusions of crystalline enstatite (*ei*). The differences between *OFC* formula of cordierite I, containing enstatite inclusions $10.0SiO_2$ $3.10Al_2O_3$ $0.30Fe_2O_3$ 3.60MgO 0.15CaO $0.19K_2O$, and *OFC* of pure cordierite $10.00SiO_2$ $3.60Al_2O_3$ $0.40Fe_2O_3$ 3.80MgO 0.20CaO (i.e., $Ca_{0.1}Mg_{1.90}Fe^{3+}{}_{0.40}Al_{3.60}Si_{5.00}O_{18}$) are relatively small.

The comparison of *OFC* formulas of amorphous phases III/1 and III/2 (variant 2 and variant 3) based on experimentally determined elemental oxides by microanalysis exhibits higher contents of Al, Fe, Mg, and Ca as compared with those calculated by variant 1 (see Appendix A), due to the zero content of Al, Fe, Mg, and Ca, which was assumed for calculation of variant 1.

The sum of percentage crystalline phases determined in variant 2 (cordierite and enstatite) is almost the same as the content of cordierite 1 (phase I) in variant 3 (Table 4). This fact is due to the simple *OFC* formulas of cordierite and enstatite identified by XRD PDF cards and used for variant 2, while cordierite variant 3 with enstatite inclusion was calculated according to the *OFC* formula in Table 3. Of course, then, the sum percentages of amorphous phase III/1 and III/2 for variant 2 and variant 3 are also the same (Table 4). Due to the heterogeneous character of III/2 phase and their higher percentages in variant 3, it is probable that this analysis is burdened by bigger errors.

CQMA (option B) is proposed as an optimized method with the aim to approximate the calculated chemical analysis ($c_{i,calc}$) from the concentrations of crystalline and amorphous phases to bulk chemical analysis ($c_{i,exp}$) of analyzed sample. The results of chemical analyses (Table 5) show this trend in all three variants 1–3. Moreover, $sumDiff^2$ (5) is calculated during the calculation of mineral contents as a control:

$$SumDiff^2 = \sum_{i=1}^{n} \left(c_{i,calc} - c_{i,exp}\right)^2 \quad (5)$$

Table 5. Recalculated mineral analyses (Table 4) on chemical analyses (wt%) by CQMA (option A) method and their comparison with bulk chemical analysis (XRF).

Oxide Elements	XRF	CQMA (Option A)		
		Variant 1	Variant 2	Variant 3
SiO_2	52.95	52.96	52.85	52.93
TiO_2	0.81	0.81	0.71	0.80
Al_2O_3	25.27	25.26	25.22	25.29
Fe_2O_3	4.44	4.39	5.28	4.43
MgO	13.26	13.24	13.41	13.27
CaO	0.70	0.77	0.63	1.97
Na_2O	0.21	0.21	0.21	0.14
K_2O	2.06	2.04	2.19	2.08
Total	99.75	99.70	100.50	99.93
Sum Diff^2		<0.01	0.77	0.08

The $sumDiff^2$ values exceeding ca. 2.0 indicate that the calculation is not fully correct or not complete, i.e., that some minor phase is not included in the calculation. More details (critical evaluation and comparison of the CQMA and QXRD-Rietveld methods of mineral phases can be found in the previous study [33]).

5. Conclusions

An innovative method based on chemical quantitative phase analysis (CQMA) was developed for the quantitative calculation of crystalline and amorphous phases for materials with simple mineral compositions. The CQMA method was tested (three different variants) on the cordierite ceramic sample CCS, prepared from a mixture of kaolinite and vermiculite at a temperature of 1300 °C. The analytical re-examination of all three variants was based on XRF chemical analysis and XRD identification of crystalline (cordierite and enstatite) and amorphous phases, with the addition of SEM/EDS for texture and microanalyses and CQMA for calculation of quantitative phase analyses.

Variant 1 calculated the maximal percentages of crystalline cordierite and enstatite and minimal amorphous phase in which Ti, Ca, K, and Na were fully fixed. Variant 2 calculated identified amorphous phases (the first III/1 with chemically homogeneous composition and the second III/2 with chemically heterogeneous one). Both their *OFC* were calculated from average microanalyses determined by EDS and from XRD PDF data of crystalline cordierite and enstatite. Variant 3 originated from the occurrence of dominant cordierite (I) containing inclusion of enstatite II and two amorphous phases III/1 and III/2 whose *OFC* were, similar to the case of variant 2, calculated from average microanalyses.

All quantitative data for three variants were finally recalculated using CQMA (option B) optimization method and a good agreement and logic relationship were revealed between their calculated contents. The results lead to the conclusion that CQMA method can also be successfully used in combination with SEM/EDS to calculate quantitative phase analysis for minerals containing chemically homogeneous amorphous phase whose crystallochemical/oxidic formula can reliably be determined.

Author Contributions: Conceptualization, Z.K. and M.V.; methodology, Z.K.; software, Z.K.; validation, Z.K. and P.M.; formal analysis, Z.K. and M.V.; investigation, Z.K. and M.V.; resources, L.B.; data curation, P.M.; writing—original draft preparation, Z.K., M.V., L.B., and P.M.; writing—review and editing L.B. and P.M. All authors have read and agreed to the published version of the manuscript.

Funding: This research was supported by the Ministry of Education, Youth and Sports of the Czech Republic under project no. CZ.02.1.01/0.0/0.0/17_049/0008426 and by the ERDF "Institute of Environmental Technology–Excellent Research", no. CZ.02.1.01/0.0/0.0/16_019/0000853.

Acknowledgments: The authors thank Dalibor Matýsek for X-ray energy dispersive spectroscopy (EDS) data.

Conflicts of Interest: The authors declare no conflict of interest. The funders had no role in the design of the study; in the collection, analyses, or interpretation of data; in the writing of the manuscript, or in the decision to publish the results.

Appendix A

Overview of used/calculated oxide formula coefficients (*OFC*) for amorphous phases for/from variants 1–3.

- Variant 1, total amorphous phase $10.0SiO_2$ $0.81TiO_2$ $0.27Na_2O$ $1.72\ K_2O$ (calculated from variant 1);
- Variants 2 and 3, amorphous phase III/1 $10SiO_2$ $0.25TiO_2$ $1.74Al_2O_3$ $0.46Fe_2O_3$ $1.08MgO$ $0.47CaO$ $0.15Na_2O$ $0.48K_2O$ (used for calculation);
- Variants 2 and 3, amorphous phase 2 (III/2) $10SiO_2$ $0.56TiO_2$ $2.66Al_2O_3$ $0.21Fe_2O_3$ $7.92MgO$ $0.10CaO$ $0.29K_2O$ (used for calculation).

References

1. Trumbulović, L.; Aćimović, Z.; Panić, S.; Andrić, L. Synthesis and characterization of cordierite from kaolin and talc for casting application. *FME Trans.* **2003**, *31*, 43–47.
2. Valášková, M. Structural characteristics of cordierites based on commercial vermiculites in relation to the natural and synthetic cordierites. *Ceram. Silikáty* **2016**, *60*, 308–316. [CrossRef]
3. Valášková, M.; Klika, Z.; Novosad, B.; Smetana, B. Crystallization and quantification of crystalline and non-crystalline phases in kaolin-based cordierites. *Materials* **2019**, *12*, 3104. [CrossRef] [PubMed]

4. Putnis, A. Order-modulated structures and the thermodynamics of cordierite reaction. *Nature* **1980**, *287*, 128–131. [CrossRef]
5. Tulyaganov, D.U.; Tukhtaev, M.E.; Escalante, J.I.; Ribeiro, M.J.; Labrincha, J.A. Processing of cordierite based ceramics from alkaline earth aluminosilicate glass, kaolin, alumina and magnesite. *J. Eur. Ceram. Soc.* **2002**, *22*, 1775–1782. [CrossRef]
6. Gregory, A.G.; Veasey, T.J. Review: The crystallisation of cordierite glass. *J. Mater Sci* **1971**, *6*, 1312–1321. [CrossRef]
7. Manchisi, J.; Matinde, E.; Rowson, N.A.; Simmons, M.J.H.; Simate, G.S.; Ndlovu, S.; Mwewa, B. Ironmaking and steelmaking slags as sustainable adsorbents for industrial effluents and wastewater treatment: A Critical review of properties, performance, challenges and opportunities. *Sustainability* **2020**, *12*, 2118. [CrossRef]
8. Shi, C. Characteristics and cementitious properties of ladle slag fines from steel production. *Cem. Concr. Res.* **2002**, *32*, 459–462. [CrossRef]
9. Kutchko, B.G.; Kim, A.G. Fly ash characterization by SEM-EDS. *Fuel* **2006**, *85*, 2537–2544. [CrossRef]
10. Wang, T.; Ishida, T.; Gu, R. A study of the influence of crystal component on the reactivity of low-calcium fly ash in alkaline conditions based on SEM-EDS. *Constr. Build. Mater.* **2020**, *243*, 118227. [CrossRef]
11. Shi, C. Steel slag—Its production, processing, characteristics, and cementitious properties. *J. Mater. Civ. Eng.* **2004**, *16*, 230–236. [CrossRef]
12. Shi, C.; Krivenko, D.R. *Alkali-Activated Cements and Concretes*, 1st ed.; Taylor & Francis: London, UK; New York, NY, USA, 2003; ISBN 9780367863630.
13. Gottlieb, P.; Wilkie, G.; Sutherland, D.; Ho-Tun, E.; Suthers, S.; Perera, K.; Jenkins, B.; Spencer, S.; Butcher, J.R. Using quantitative electron microscopy for process mineralogy applications. *JOM* **2000**, *52*, 24–25. [CrossRef]
14. Leng, Y. *Material Characterization: Introduction to Microscopic and Spectroscopic Methods*, 2nd ed.; Wiley: Hoboken, NJ, USA, 2008; ISBN 978-3-527-33463-6.
15. Ziel, R.; Haus, A.; Tulke, A. Quantification of the pore size distribution (porosity profiles) in microfiltration membranes by SEM, TEM and computer image analysis. *J. Membr. Sci.* **2008**, *323*, 241–246. [CrossRef]
16. Hodoroaba, V.D.; Rades, S.; Unger, W.E.S. Inspection of morphology and elemental imaging of single nanoparticles by high resolution SEM/EDX in transmission mode. *Surf. Intersurf. Anal.* **2014**, *46*. [CrossRef]
17. Shindo, D.; Oikawa, T. Energy dispersive X-ray spectroscopy. In *Analytical Electron Microscopy for Materials Science*; Springer: Tokyo, Japan, 2002. [CrossRef]
18. Newburry, D.E.; Ritchie, N.W.M. is scanning electron microscopy/energy dispersive X-ray spectrometry (SEM/EDS) quantitative? *J. Scanning Microsc.* **2012**, *35*. [CrossRef]
19. Dinnebier, R.E.; Billinge, S.J.L.; Garnier, E. *Powder Diffraction Theory and Practice*; RSC Publishing: Cambridge, UK, 2009; ISBN 9781847558237.
20. Rietveld, H.M. Line profiles of neutron powder-diffraction peaks for structure refinement. *Acta Crystallographica* **1967**, 151–152. [CrossRef]
21. Bish, L.; Post, J.E. *Modern Powder Diffraction*; Mineralogical Society of America: Washington, DC, USA, 1989; ISBN 0939950243.
22. Young, R.A. *The Ritveld Method*; Oxford University Press: Oxford, UK, 1995; ISBN 0198559127.
23. Kemethmüller, S.; Roosen, A.; Goetz-Neunhoeffer, F.; Neubauer, J. Quantitative analysis of crystalline and amorphous phases in glass-ceramic composites like LTCC by the Rietveld method. *J. Am. Ceram. Soc.* **2006**, *89*. [CrossRef]
24. Zhao, P.; Lu, L.; Liu, X.; De la Torre, A.G.; Cheng, X. Error analysis and correction for quantitative phase analysis based on Rietveld-internal standard method: Whether the minor phases can be ignored? *Crystals* **2018**, *8*, 110. [CrossRef]
25. Chancey, R.T.; Stutzman, P.; Juenger, M.; Fowler, D. Comprehensive phase characterization of crystalline and amorphous phases of a Class F fly ash. *Cem. Concr. Res.* **2010**, *40*, 146–156. [CrossRef]
26. García-Maté, M.; Santacruz, I.; Cuesta, A.; León-Reina, L.; Aranda, M.A.G.; Baco, I.; Morin, V.; Walenta, G.; Gartner, E.; De la Torre, A.G. Amorphous determination in calcium sulfoaluminate materials by external and internal method. *Adv. Res.* **2015**, *27*, 417–423. [CrossRef]
27. Madsen, I.; Scarlett, N.; Kern, A. Description and survey of methodologies for the determination of amorphous content via X-ray powder diffraction. *Zeitschrift Kristallographie* **2011**, *226*, 944–955. [CrossRef]
28. Hodgson, M.; Dudeney, A.W.L. Estimation of clay proportions in mixtures by X-Ray diffraction and computerized chemical mass balance. *Clays Clay Miner.* **1984**, *32*, 19–28. [CrossRef]

29. Johnson, L.J.; Chu, C.H.; Hussey, G.A. Quantitative clay mineral analysis using simultaneous linear equations. *Clays Clay Miner.* **1985**, *33*, 107–117. [CrossRef]
30. Braun, G.E. Quantitative analysis of mineral mixtures using linear programming. *Clays Clay Miner.* **1986**, *34*, 330–337. [CrossRef]
31. Whiten, B. Calculation of mineral composition from chemical assays. *Miner. Process. Extr. Metall. Rev.* **2007**, *29*, 83–97. [CrossRef]
32. Coelho, C.; Roqueiro, D.; Hotza, D. Rational mineralogical analysis of ceramics materials. *Letters* **2002**, *52*, 394. [CrossRef]
33. Klika, Z.; Kolomazník, I.; Matýsek, D.; Kliková, C. Critical evaluation of a new method for quantitative determination of minerals in solid samples. *Cryst. Res. Technol.* **2016**, *51*, 249–264. [CrossRef]
34. Hillier, S. Accurate quantitative analysis of clay and other minerals in sandstones by XRD: Comparison of a Rietveld and a reference intensity ratio (RIR) method and the importance of sample preparation. *Clay Miner.* **2000**, *35*, 291–302. [CrossRef]
35. Balasone, G.; Franco, E.; Mattia, C.A.; Puliti, R. Indialite in xenolithic rocks from Somma-Vesuvius volcano (Southern Italy): Crystal chemistry and petrogenetic features. *Am. Mineral.* **2004**, *89*, 1–6. [CrossRef]